

## ORIGINAL MANUSCRIPT

# Loss of Snail2 favors skin tumor progression by promoting the recruitment of myeloid progenitors

Ana Villarejo<sup>1</sup>, Patricia Molina-Ortiz<sup>1,6</sup>, Yenny Montenegro<sup>1</sup>,  
Gema Moreno-Bueno<sup>1,2</sup>, Saleta Morales<sup>1</sup>, Vanesa Santos<sup>1</sup>, Tom Gridley<sup>3</sup>,  
Mirna A. Pérez-Moreno<sup>4</sup>, Héctor Peinado<sup>5,7</sup>, Francisco Portillo<sup>1</sup>,  
Carmela Calés<sup>1</sup> and Amparo Cano<sup>1,\*</sup>

<sup>1</sup>Departamento de Bioquímica, Universidad Autónoma de Madrid: Instituto de Investigaciones Biomédicas “Alberto Sols” CSIC-UAM; IdiPAZ, Madrid 28029, Spain, <sup>2</sup>Fundación MD Anderson International Madrid, Madrid 28033, Spain, <sup>3</sup>Center for Molecular Medicine, Maine Medical Center Research Institute, Scarborough, ME 04074, USA, <sup>4</sup>Cancer Biology Program, Centro Nacional de Investigaciones Oncológicas, Madrid 28029, Spain and <sup>5</sup>Department of Pediatrics, Cell and Developmental Biology, Weill Cornell Medical College, New York, NY 10021, USA

<sup>6</sup>Present address: Laboratory of Functional Genetics, GIGA Research Centre, Université de Liège, Avenue de l’Hôpital n°1 (B34), 4000-Liège, Belgium. <sup>7</sup>Present address: Centro Nacional de Investigaciones Oncológicas (CNIO), Madrid 28029, Spain.

\*To whom correspondence should be addressed. Tel: +34 9149 75400; Fax: +34 9158 54401; Email: [acano@iib.uam.es](mailto:acano@iib.uam.es)

## Abstract

Snail2 is a zinc finger transcription factor involved in driving epithelial to mesenchymal transitions. *Snail2* null mice are viable, but display defects in melanogenesis, gametogenesis and hematopoiesis, and are markedly radiosensitive. Here, using mouse genetics, we have studied the contributions of Snail2 to epidermal homeostasis and skin carcinogenesis. *Snail2*<sup>-/-</sup> mice presented a defective epidermal terminal differentiation and, unexpectedly, an increase in number, size and malignancy of tumor lesions when subjected to the two-stage mouse skin chemical carcinogenesis protocol, compared with controls. Additionally, tumor lesions from *Snail2*<sup>-/-</sup> mice presented a high inflammatory component with an elevated percentage of myeloid precursors in tumor lesions that was further increased in the presence of the anti-inflammatory agent dexamethasone. *In vitro* studies in *Snail2* null keratinocytes showed that loss of Snail2 leads to a decrease in proliferation indicating a non-cell autonomous role for Snail2 in the skin carcinogenic response observed *in vivo*. Bone marrow (BM) cross-reconstitution assays between *Snail2* wild-type and null mice showed that Snail2 absence in the hematopoietic system fully reproduces the tumor behavior of the *Snail2* null mice and triggers the accumulation of myeloid precursors in the BM, blood and tumor lesions. These results indicate a new role for Snail2 in preventing myeloid precursors recruitment impairing skin chemical carcinogenesis progression.

## Introduction

The Snail2 (Slug) protein belongs to the Snail superfamily of zinc finger transcription factors, characterized by their ability to induce epithelial to mesenchymal transition (EMT) (1–3). This developmental program is characterized by the loss of apico-basal polarity, decreased expression of epithelial markers such as E-cadherin and the acquisition of mesenchymal

properties, including expression of vimentin and an increase in invasive capability (1,3). In development, both EMT and the reverse process, mesenchymal to epithelial transition, are essential for cells to retain their plasticity and the ability to switch between different morphological states in response to physiological cues (2).

Received: July 3, 2014; Revised: February 26, 2015; Accepted: March 6, 2015

© The Author 2015. Published by Oxford University Press. All rights reserved. For Permissions, please email: [journals.permissions@oup.com](mailto:journals.permissions@oup.com).

**Abbreviations:**

BM	bone marrow
BrdU	Bromodeoxyuridine
DMBA	7,12-dimethylbenzanthracene
EMT	epithelial to mesenchymal transition
H&E	hematoxylin and eosin
HF	hair follicle
IMC	immature myeloid cell
OCT	optimal cutting temperature
PBS	phosphate-buffered saline
SCC	squamous cell carcinoma
TPA	12-O-tetradecanoylphorbol-13-acetate

Snail factors play differential roles in the development of different species (4). In the mouse embryo, *Snail1* expression is restricted to specific EMT areas, whereas *Snail2* is expressed at high levels in several tissues like craniofacial mesenchyme and the stomach wall (4,5). In addition, *Snail2* is expressed in adult tissues (6), such as basal cells of various stratified, and pseudostratified epithelia including hair follicles (HFs) and the interfollicular epidermis (7). *Snail2* also has an important role in skin homeostasis and in wound healing, where its expression rises at the border of the injury (8,9). Furthermore, keratinocyte outgrowth is impaired in skin explants derived from *Snail2*<sup>-/-</sup> mice (10). These data support a role for *Snail2* in re-epithelialization (8,10), a process reminiscent of a partial EMT (3). Moreover, after ultraviolet radiation, *Snail2* is able to induce an acute response in keratinocytes (11).

In contrast to *Snail1* null mice that are embryonic lethal (12), *Snail2* null mice are viable, although they display some abnormalities like small body size, reduced fertility, craniofacial defects, pigmentary alterations, macrocytic anemia and increased apoptosis in the thymic cortex (13). In addition, *Snail2* null mice are born below the expected Mendelian ratio due to embryonic defects in palatal closure and low perinatal survival (unpublished observations). Furthermore, *Snail2*<sup>-/-</sup> mice are much more radiosensitive than wild-type mice, showing a decrease in peripheral blood cells, increase in microhemorrhages and bacterial microabscesses under ultraviolet light (14–16). The absence of *Snail2* does not modify the physiological homeostasis of bone marrow (BM) stem cells; however, extramedullary repopulation is enhanced under hematopoietic stress in *Snail2* null mice (17). In addition, *Snail2* is a target of the stem cell factor/c-kit pathway (15,16), which is essential for hematopoiesis, melanogenesis and gametogenesis.

The pro-migratory and pro-invasive properties acquired by cells that have undergone an EMT have established this process as a key mechanism by which tumor cells achieve properties that allow them to leave the primary tumor site, thus favoring the initiation of the metastatic process (3,18,19). *Snail2* promotes EMT by binding to the E-cadherin promoter and repressing its expression in epithelial cells, accompanied by changes in cell morphology (20–22). *Snail2* has been involved in different cancer types and is considered a marker of malignancy (23,24). In human tumor samples, *Snail2* expression has been associated with breast carcinoma recurrence and metastasis (25), and with lymph node metastasis and poor prognosis in squamous cell carcinoma (SCC) (26). Moreover, *Snail2* has been related with mammary cancer stem cell function (27,28) and survival during metastasis (29). However, *in vivo* data concerning *Snail2* function are scarce, despite the relevance of *Snail2* in tumor progression.

In the present work, we have analyzed in detail the *in vivo* role of *Snail2* in skin homeostasis and skin chemical carcinogenesis

in mice with constitutive *Snail2* deletion. We show that *Snail2* is required for proliferation and terminal differentiation of keratinocytes but, unexpectedly, impairs skin tumor progression and inflammation. To assess the specific contribution of hematopoietic precursors to tumor progression, hematopoietic cross-reconstitution was performed between *Snail2* wild-type and null mice. Our results show that *Snail2* deletion in the hematopoietic system triggers tumor progression through accumulation of myeloid precursors in the lesions, concomitant to activation of the Wnt/ $\beta$ -catenin pathway. Our results suggest that *Snail2* prevents inflammation-dependent malignant progression in skin tumors.

**Materials and methods****Snail2 null mice**

*Snail2*<sup>+/-</sup> heterozygous mice were generated and provided by T. Gridley (13) on the C57BL6 genetic background. Due to the poor postnatal survival of *Snail2*<sup>-/-</sup> null mice on this background, *Snail2*<sup>+/-</sup> heterozygotes were backcrossed onto the Friend virus B-type background for three generations before being intercrossed to generate *Snail2*<sup>-/-</sup>, *Snail2*<sup>+/-</sup> and *Snail2*<sup>+/+</sup> mice. Survival of *Snail2*<sup>-/-</sup> mice in the mixed background slightly increased to 2–5% of pups from heterozygous breedings. The *Snail2* null allele contains a substitution of the zinc finger region by the reporter gene *LaZ*, so the transgene expression encodes a functional  $\beta$ -galactosidase enzyme (13). *Snail2*<sup>-/-</sup>, *Snail2*<sup>+/-</sup> and *Snail2*<sup>+/+</sup> mice were used for all the experiments at 6–8 weeks of age. All experiments were performed according to the institutional proceedings for animal experimentation approved by the Universidad Autónoma de Madrid ethics committee (CEI-25-587).

**12-O-tetradecanoylphorbol-13-acetate-induced hyperproliferation and wound healing assays**

Six-week-old *Snail2*<sup>+/+</sup>, *Snail2*<sup>+/-</sup> and *Snail2*<sup>-/-</sup> mice were shaved in the dorsal skin the day prior to treatment. Topical applications of 12-O-tetradecanoylphorbol-13-acetate (TPA) (P8139; Sigma) (20nM in 200  $\mu$ l of acetone) were administered on the dorsal skin of the mouse every 2 days for 1 week, then the dorsal skin was removed, fixed in formaldehyde, sectioned and the slides obtained were stained with hematoxylin and eosin (H&E). For wound healing assays, an incision with a 10mm diameter punch was performed on the dorsal skin, and the diameter of the wound was measured everyday during 2 weeks until it was completely closed.

**Bromodeoxyuridine labeling**

Three-day-old mice were injected twice daily for 3 days with bromodeoxyuridine (BrdU) at 50  $\mu$ g/dose, for a cumulative daily dose of 100  $\mu$ g. Skins were collected 7 weeks after administering the last dose to assess the localization of label retaining cells under steady-state conditions. The localization of label retaining cells in the BrdU-stained tissues was assessed using fluorescent microscopy.

**'Clipping' assay**

*Snail2*<sup>+/+</sup>, *Snail2*<sup>+/-</sup> and *Snail2*<sup>-/-</sup> mice at P20, P50 and P90 were shaved and observed daily until the hair appeared again in at least one of the mouse genotypes. At the end of the experiment, the dorsal skin was collected and divided in several portions for freezing and RNA extraction or fixed in formaldehyde. Paraffin and optimal cutting temperature (OCT) sections were obtained to analyze the samples by H&E and immunofluorescence.

**7,12-Dimethylbenzanthracene/TPA and dexamethasone treatment**

The mice dorsal skin was shaved 1 day before topical application of a single dose of 7,12-dimethylbenzanthracene (DMBA) (Sigma-Aldrich) (200  $\mu$ l of a dilution at 160  $\mu$ g/ml). Seven days after initiation, the dorsal skin was treated twice weekly with the tumor promoter TPA (20nM in 200  $\mu$ l of acetone) for 16 weeks and the mice were followed for 18–22 weeks. When indicated mice were daily injected with dexamethasone [0.05 mg/kg diluted in phosphate-buffered saline (PBS) from a 100 $\times$  stock solution

in ethanol] from 12 weeks post-initiation to the end of the carcinogenesis experiment. Control groups were treated with PBS. The number of skin lesions per mouse was measured with a caliper once a week. All the lesions were examined histologically on H&E-stained paraffin sections for detailed diagnosis.

### BM reconstitution

For BM reconstitution, mice with the different *Snail2* genotypes were irradiated with 10 Gy (lethal dose, wild-type and heterozygous animals) or 6 Gy (sublethal dose, homozygous *Snail2*<sup>-/-</sup> mice) using a Cs-137 Shepherd Mark I-30 gamma-irradiator and injected with 5 × 10<sup>6</sup> total BM cells isolated from mice with the corresponding genotypes: *Snail2*<sup>+/+</sup><sub>BMSnail2</sub><sup>+/+</sup>, *Snail2*<sup>+/+</sup><sub>BMSnail2</sub><sup>-/-</sup>, *Snail2*<sup>-/-</sup><sub>BMSnail2</sub><sup>+/+</sup>, *Snail2*<sup>-/-</sup><sub>BMSnail2</sub><sup>-/-</sup>. One month later, blood samples were obtained to perform PCR analyses of *Snail2* and *LacZ* genes to assess the occurrence of an effective hematopoietic repopulation. DMBA/TPA treatment was then started.

### Histological procedures, H&E staining and immunohistochemistry

Samples obtained from *in vivo* assays were fixed in 3.7% formaldehyde or frozen with liquid nitrogen to generate paraffin and OCT (Takara) blocks, respectively, as described previously (30).

H&E stainings were performed using paraffin sections as described previously (30). Immunohistochemical stainings on 4 μm paraffin sections with the indicated antibodies (Supplementary Table S1, available at *Carcinogenesis* Online) were performed using the LSAB (Dako) method with a heat-induced antigen retrieval step (30).

### β-Galactosidase assay

β-Galactosidase activity was determined in 5 μm OCT skin sections. Briefly, samples were treated with 1% paraformaldehyde pH 7.4, 0.2% glutaraldehyde and 0.02% NP-40 for 1 h at 4°C, followed by washing (×2) 20 min in PBS/0.02% NP-40. Samples were then incubated in 5 mM C<sub>6</sub>H<sub>5</sub>FeK<sub>3</sub>, 2 mM MgCl<sub>2</sub>, 0.02% NP-40 and 1 mg/ml X-gal for 24 h at room temperature and viewed under an Olympus microscope equipped with a CCD Olympus DP70 digital camera.

### Western blot

Cell extracts were obtained from skin of 8-week-old mice from the three *Snail2* genotypes. Briefly, tissue disaggregation was performed with an electric homogenizer and 500 μl of RIPA buffer (0.1% sodium dodecyl sulfate, 0.5% sodium deoxycholate, 1% NP-40, 150 mM NaCl, 50 mM Tris-HCl pH 8.0) containing protease inhibitors. Extracts were centrifuged for 20 min at 13000 r.p.m. at 4°C, and supernatants were collected. Protein samples were resolved on sodium dodecyl sulfate-polyacrylamide gel electrophoresis, transferred to nitrocellulose Immobilon-P membranes (Millipore) and analyzed by western blot as described (30). Briefly, membranes were blocked using 5% non-fat dry milk in 0.5% Tween-Tris glycine buffer and then incubated at 4°C overnight with anti-*Snail2* antibody (Santa Cruz, 1:1000) followed by 1 h incubation at room temperature with horseradish peroxidase-coupled goat anti-rabbit (Pierce, 1:10000). After washings, proteins were resolved with ECL detection reagent (Amershan).

### Immunofluorescence and terminal deoxynucleotidyl transferase-mediated dUTP nick end labeling assays

Five micrometer OCT sections were treated with 1% paraformaldehyde for 20 min at room temperature and then permeabilized for 15 min at room temperature with 0.05% Triton X-100 and washed with PBS. Samples were then blocked with 2% bovine serum albumin in PBS, incubated with primary antibodies for 1 h, washed and incubated with the correspondent secondary antibodies. Antibody information is supplied in Supplementary Table S1, available at *Carcinogenesis* Online. For terminal deoxynucleotidyl transferase-mediated dUTP nick end labeling assays, OCT sections were fixed with 4% paraformaldehyde for 20 min, washed with PBS for 30 min and permeabilized with 0.1% sodium citrate, 0.1%

Triton X-100 for 2 min at 4°C and stained with *In situ* cell death detection kit (Roche), following the manufacturer's instructions. Nuclei were stained with 4',6-diamidino-2-phenylindole (Molecular Probes, 1:5000) and samples were mounted with Mowiol (Sigma-Aldrich). Images were acquired with a Nikon 90i microscope equipped with a CCD Olympus DP70 camera or in a Leica LSP confocal microscope and processed with Adobe Photoshop CS.

### Keratinocyte culture

The skin from newborn mice was treated with trypsin 0.25% at 4°C for 16 h to separate the epidermis from the dermis. The epidermis was disaggregated and filtered through a 40 μm filter (BD Falcon) and primary keratinocytes were seeded in MW96 plates (Falcon), previously covered with NIH3T3 feeder cells and grown in DMEM:F12 (3:1) pH 7.2 medium, containing 15% fetal bovine serum (Gibco) treated with CHELEX (Bio-Rad), hydrocortisone, choleric toxin, transferrin, insulin, thyronine (Sigma), 0.3 mM CaCl<sub>2</sub>, 100 μg/ml ampicillin and 32 μg/ml gentamicin (Gibco). Primary cultures were maintained for 10 days until colony formation and were classified by size and morphology.

### Flow cytometry

Blood and BM samples were collected, centrifuged at 150g for 5 min and washed with PBS. Tumor samples were disaggregated mechanically and filtered through 40 μm filters. Then, cells were incubated with the indicated antibodies (Supplementary Table S1, available at *Carcinogenesis* Online) and washed with 1× PBS. Propidium iodide was added to discard dead cells. Samples were acquired in a Cytomics FC 500 MPL equipment, and data analyzed with the CXP software (Beckman-Coulter).

### PCR and quantitative PCR analyses

Blood DNA was isolated from BM transplanted animals 1 month after transplantation by extraction with organic extraction method. Twenty nanograms of DNA was analyzed by PCR for *Snail2* and *LacZ* detection. cDNA from the different samples was obtained from 1 μg of total RNA using random primers and Superscript II system (Life Technologies Inc.) as described previously (29). Quantitative real-time PCR was performed with an iQ5 BIORAD machine (Bio-Rad Laboratories SA), using Sybergreen and the manufacturer's recommended conditions. The comparative threshold cycle (Ct) method was used to calculate the amplification factor. Primer sequences are detailed in Supplementary Table S2, available at *Carcinogenesis* Online.

### Statistics

Error bars in the graphical data represent mean ± SD. P values of P < 0.05 were considered statistically significant by two-tailed Student's *t*-test. To test associations between categorical variables, we used the χ<sup>2</sup> or Fisher's exact test. Values of P < 0.05 were considered statistically significant. Statistical analysis was performed using SPSS 17.0 program (SPSS Inc., Chicago, IL).

## Results

### *In vivo* *Snail2* function in epidermal proliferation and differentiation

*Snail2* ablation in skin of null and heterozygous mice was confirmed by analyzing β-galactosidase activity (Figure 1A) also showing that *Snail2* is expressed in the interfollicular epidermis and prominently in the HFs, including the bulge region where epidermal stem cells are located (Figure 1A). Immunohistochemical analysis confirmed *Snail2* protein nuclear expression in those epidermal areas in control mice, whereas no expression was detected in *Snail2*<sup>-/-</sup> mice (Figure 1B). Western blot and quantitative PCR assays further confirmed the absence of *Snail2* at protein and mRNA level in skin from *Snail2*<sup>-/-</sup> mice and intermediate levels in *Snail2*<sup>+/-</sup> compared with wild-type mice (Figure 1C and Supplementary

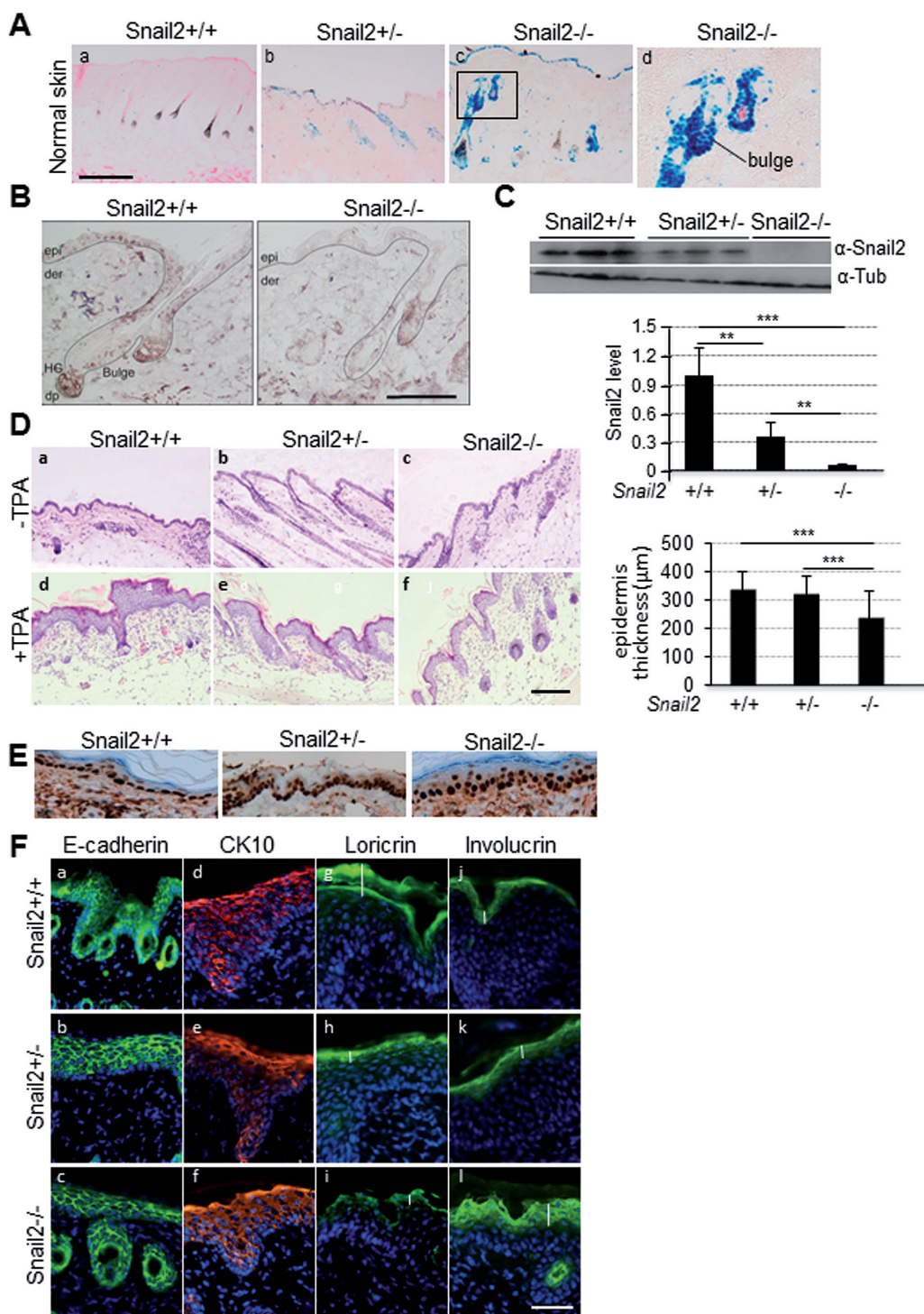


**Figure 1.** Analysis of Snail2 in skin homeostasis. (A) Skin  $\beta$ -galactosidase staining as an indicator of Snail2 ablation in Snail2<sup>-/-</sup> (b) and Snail2<sup>-/-</sup> (c and d) mice; skin from Snail2<sup>+/+</sup> mice (a) is shown as a negative control. Bar, 500  $\mu$ m. (B) Snail2 immunohistochemistry from Snail2<sup>+/+</sup> and Snail2<sup>-/-</sup> mice skin. (C) Snail2 western blot in skin from the indicated Snail2 genotypes;  $\beta$ -tubulin was used as loading control. Quantitation of the relative Snail2 levels is shown in the lower diagram. (D) H&E images from TPA-treated and control skin. Bar, 200  $\mu$ m. Quantitation of epidermal thickness in the three Snail2 genotypes after TPA treatment is shown in the right diagram. (E) Proliferating cell nuclear antigen immunohistochemistry from untreated Snail2<sup>+/+</sup>, Snail2<sup>+/-</sup> and Snail2<sup>-/-</sup> mice skin. (F) Immunofluorescence analysis for the expression of E-cadherin, CK10, loricrin and involucrin in Snail2<sup>+/+</sup>, Snail2<sup>+/-</sup> and Snail2<sup>-/-</sup> skin after TPA treatment. Nuclei were stained with 4',6-diamidino-2-phenylindole (blue). Bar, 200  $\mu$ m. Vertical white bars in panels g-l denote the extension of loricrin and involucrin stain in TPA-treated skins from the indicated Snail2 genotypes. \*\*\* $P < 0.001$ .

Figure S1A, available at Carcinogenesis Online). To analyze the *in vivo* proliferative capacity of keratinocytes, Snail2<sup>-/-</sup>, Snail2<sup>+/-</sup> and control wild-type mice were treated with TPA on the dorsal skin for 1 week and the thickness of the epidermis

was analyzed in H&E sections (Figure 1D). The hyperplasia of the skin caused by the TPA treatment was less prominent in Snail2<sup>-/-</sup> compared with Snail2<sup>+/+</sup> and Snail2<sup>+/-</sup> mice (Figure 1D, right panel). Proliferating cell nuclear antigen staining of skins

from untreated mice revealed no significant differences in the epidermal proliferative capacity of *Snail2*<sup>-/-</sup> compared with the other two genotypes (Figure 1E). On the other hand, *in vivo* wounding assays showed that the time required for healing was significantly delayed during the first 2 days in *Snail2*<sup>-/-</sup> regarding control and *Snail2*<sup>+/-</sup> mice (Supplementary Figure S2, available at Carcinogenesis Online), in agreement with previous observations (8,10). We then analyzed whether *Snail2* deletion affects the differentiation of TPA-treated skin by staining for E-cadherin, suprabasal (CK10) and terminal differentiation markers (loricrin and involucrin) (Figure 1F). No major differences in the expression of E-cadherin (Figure 1F, a–c) and CK10 (Figure 1F, d–f) could be detected among the different *Snail2* genotypes, but the loricrin and involucrin expression patterns were altered in the *Snail2*<sup>-/-</sup>-treated skin. Loricrin expression was apparently decreased and restricted to the most external layer, whereas involucrin was expanded to additional suprabasal layers, with a more diffuse pattern in *Snail2*<sup>-/-</sup> compared with *Snail2*<sup>+/+</sup> and *Snail2*<sup>+/-</sup> mice (Figure 1F, g–l).

These results suggest a defect in the terminal differentiation of *Snail2*<sup>-/-</sup> epidermis in response to proliferative stresses and point to a potential involvement of *Snail2* in the *in vivo* proliferation of epidermal keratinocytes under those conditions.

### Snail2 deletion promotes skin tumor progression

SNAI2 has been proposed as a prognostic marker in esophageal SCC (26). Therefore, we decided to study the functional implication of *Snail2* in epidermal tumor formation and progression by analyzing the response of *Snail2*<sup>+/+</sup>, *Snail2*<sup>-/-</sup> and *Snail2*<sup>+/-</sup> mice to the classical chemical skin carcinogenesis protocol (DMBA/TPA). The results showed that mice from all genotypes have a similar tumor incidence although the *Snail2*<sup>+/-</sup> mice showed a delayed time to reach 100% incidence compared with *Snail2* wild-type and null mice (Figure 2A). One prominent difference in the tumor behavior among the three *Snail2* genotypes concerned the emergence and number of lesions. *Snail2*<sup>-/-</sup> and *Snail2*<sup>+/-</sup> mice developed fewer lesions than *Snail2*<sup>+/+</sup> mice at the initial stages of skin carcinogenesis (up to 12 weeks), denoting relevant differences in the latency period in the partial or total absence of *Snail2*. Unexpectedly, after 13 weeks post-initiation, the number of lesions in *Snail2*<sup>-/-</sup> mice was markedly and progressively increased compared with *Snail2*<sup>+/+</sup> and *Snail2*<sup>+/-</sup> mice (Figure 2B). At week 20, the number of lesions in *Snail2*<sup>-/-</sup> mice were significantly increased reaching an average of 20 lesions/mouse compared with *Snail2*<sup>+/+</sup> and *Snail2*<sup>+/-</sup> with an average of 10 and 5 lesions/mouse, respectively (Figure 2B). Moreover, *Snail2*<sup>-/-</sup> mice developed significantly larger lesions than wild-type and *Snail2*<sup>+/-</sup> mice all along the experimental time course (Figure 2C and Supplementary Table S3, available at Carcinogenesis Online).

Histopathological analysis revealed that DMBA/TPA treatment mostly triggers the development of papillomas and some hyperplasias in the three *Snail2* genotypes. Surprisingly, the percentage of SCC in *Snail2*<sup>-/-</sup> mice was markedly increased (31%) compared with *Snail2*<sup>+/+</sup> (7%) and *Snail2*<sup>+/-</sup> (4%) mice (Figure 2D). The increase in SCC in *Snail2*<sup>-/-</sup> mice is related with the decrease in papillomas (63% in *Snail2*<sup>-/-</sup> versus 82% in *Snail2*<sup>+/+</sup> and 96% in *Snail2*<sup>+/-</sup> mice). These results suggest that *Snail2* ablation has a dual role in tumors, in one hand it delays tumor initiation, and in the other one, it increases the tumor burden and malignancy of the lesions at late carcinogenic stages. Interestingly, the absence of a single *Snail2* allele impairs both tumor initiation and progression.

### Snail2 deletion modifies the expression pattern of papilloma markers toward a pre-malignant profile

To investigate the potential role of *Snail2* in the proliferation status of tumor lesions, we first examined the expression of proliferation (cyclin D1) and basal progenitor cells (p63) markers by immunohistochemistry as well as apoptosis (terminal deoxynucleotidyl transferase-mediated dUTP nick end labeling) in papillomas and SCCs. *Snail2*<sup>-/-</sup> lesions showed increased cyclin D1 (Figure 2E, panels a–c and g–i) and p63 staining (Figure 2E, d–f) compared with the other two genotypes, suggesting a higher proliferative potential and less differentiated status of lesions derived from *Snail2* null mice. Terminal deoxynucleotidyl transferase-mediated dUTP nick end labeling assay indicated the presence of an increased number of apoptotic cells in papillomas from *Snail2*<sup>-/-</sup> and *Snail2*<sup>+/-</sup> compared with wild-type lesions (Figure 2F, a–c), in agreement with *Snail2* protective action against cell death after genotoxic stress (14,16). These data, nevertheless, indicated that the increased proliferation observed in *Snail2*<sup>-/-</sup> lesions is not compensated by apoptosis. Because of the key role ascribed to the Wnt/ $\beta$ -catenin pathway in skin tumor progression (31,32) and the reported correlation between p63 and  $\beta$ -catenin levels (33), we speculated that  $\beta$ -catenin expression/activation could be altered in tumor lesions from *Snail2* deficient mice. Immunofluorescence analyses showed that *Snail2*<sup>-/-</sup> papillomas displayed cytoplasmic  $\beta$ -catenin in contrast to *Snail2*<sup>+/-</sup> and *Snail2*<sup>+/+</sup> lesions (Figure 2F, d–f). Complementary, immunohistochemical analyses indicated that only *Snail2*<sup>-/-</sup> papillomas show  $\beta$ -catenin nuclear localization and more cytoplasmic presence compared with *Snail2*<sup>+/+</sup> and *Snail2*<sup>+/-</sup> papillomas (Figure 2F, g–i). Analysis of different components of the Wnt/ $\beta$ -catenin pathway in *Snail2*<sup>+/+</sup> and *Snail2*<sup>-/-</sup> papillomas showed increased expression of Wnt ligands, mainly Wnt4, and periostin (POSTN), a Wnt agonist (34), in *Snail2*<sup>-/-</sup> lesions (Supplementary Figure S3, available at Carcinogenesis Online). Together, these data suggest an increased activation of the Wnt/ $\beta$ -catenin pathway, which may contribute to the progression of *Snail2*<sup>-/-</sup> papilloma to a premalignant state.

To ascertain the differentiation status of the lesions, we next investigated the expression pattern of the established differentiation markers loricrin, CK10, CK13 and CK8 in papillomas and SCC from the three *Snail2* genotypes by immunohistochemistry. Loricrin was expressed in the upper suprabasal layers of papillomas with a more extended pattern in *Snail2*<sup>-/-</sup> lesions (Figure 3A, d–f) and maintained at low levels in *Snail2*<sup>-/-</sup> SCC in contrast to its absence in *Snail2*<sup>+/+</sup> and *Snail2*<sup>+/-</sup> SCC (Figure 3B, d–f), suggesting that terminal differentiation of *Snail2*<sup>-/-</sup> lesions is altered, consistent with the results previously observed upon treating the skin with TPA. CK10, a marker of papilloma differentiation, is expressed in the suprabasal layers of papillomas and at low levels in SCC from *Snail2*<sup>+/+</sup> mice (Figure 3A and B, panel g) while strongly decreased or absent in *Snail2*<sup>-/-</sup> (Figure 3A and B, h) and *Snail2*<sup>+/-</sup> lesions (Figure 3A and B, i). CK13, an early marker of papilloma progression (35), was highly expressed even in well-differentiated papillomas from *Snail2*<sup>+/-</sup> (Figure 3A, k) and *Snail2*<sup>+/+</sup> mice (Figure 3A, l), in contrast to its almost complete absence in wild-type papillomas (Figure 3A, j). Moreover, high expression levels of CK13 were maintained in SCC from *Snail2*<sup>-/-</sup> compared with SCC from *Snail2*<sup>+/-</sup> and *Snail2*<sup>+/+</sup> mice (Figure 3B, j–l). On the other hand, the expression of CK8, a marker of progression from papilloma to SCC (36), showed a similar pattern to CK13 being expressed in papillomas from *Snail2*<sup>-/-</sup> and *Snail2*<sup>+/-</sup> mice

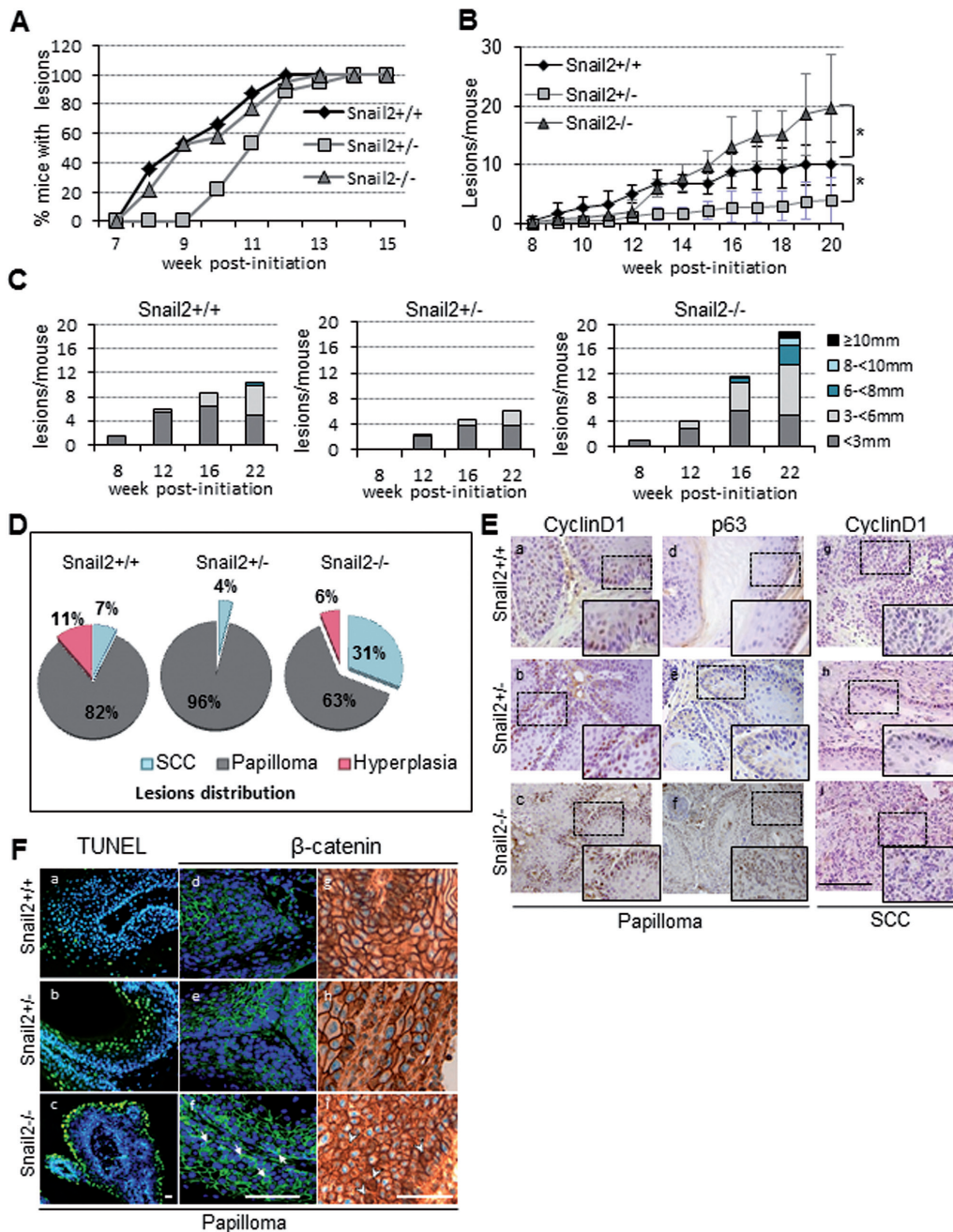


**Figure 2.** Effect of *Snail2* constitutive deletion in DMBA/TPA skin carcinogenesis. (A) Incidence and time of appearance of first lesions in *Snail2*<sup>+/+</sup> (*n* = 13), *Snail2*<sup>+/-</sup> (*n* = 10) and *Snail2*<sup>-/-</sup> (*n* = 13) mice. (B) Tumor burden indicated as the mean number of lesions/mouse in the three *Snail2* genotypes. (C) Tumor size represented as the mean number of lesions per mouse reaching the indicated diameter at week 8, 12, 16 and 22 post-initiation. (D) Distribution in percentage of lesions in *Snail2*<sup>+/+</sup>, *Snail2*<sup>+/-</sup> and *Snail2*<sup>-/-</sup> mice classified as hyperplasia, papilloma or SCC. (E) Immunohistochemical analysis of cyclin D1 and p63 of *Snail2*<sup>+/+</sup>, *Snail2*<sup>+/-</sup> and *Snail2*<sup>-/-</sup> papillomas (a-f) and SCC (g-i). Bar, 500 μm. Amplified images of the indicated areas (squares) are included as insets. (F) Apoptosis (a-c) measured by terminal deoxynucleotidyl transferase-mediated dUTP nick end labeling assay and β-catenin immunofluorescence (d-f) and immunohistochemical (g-i panels) staining of *Snail2*<sup>+/+</sup>, *Snail2*<sup>+/-</sup> and *Snail2*<sup>-/-</sup> papillomas. Nuclei were stained with 4',6-diamidino-2-phenylindole (blue). White arrows (f) and arrowheads (i) denote cytoplasmic and/or nuclear localization of β-catenin in *Snail2*<sup>-/-</sup> papillomas. Bar, 100 μm.

(Figure 3A, n, o) and at higher levels in SCCs from *Snail2*<sup>-/-</sup> mice (Figure 3B, o). Collectively, these data indicate that *Snail2*<sup>-/-</sup> papillomas are less differentiated and more prone to progress to SCC than those generated from the *Snail2*<sup>+/-</sup> and *Snail2*<sup>+/+</sup> mice, in agreement with the increased number of SCC observed in the *Snail2* null phenotype. Interestingly, although *Snail2*<sup>+/-</sup> papillomas show a marker expression consistent with low differentiation, they hardly progress into SCC, suggesting

that absence of a single *Snail2* allele prevents additional events required for tumor progression.

#### **Snail2 deletion promotes tumor progression by non-cell autonomous mechanisms**

The increased proliferation and malignant progression of skin lesions from *Snail2* null mice could be caused by keratinocyte intrinsic mechanisms and/or interactions with the

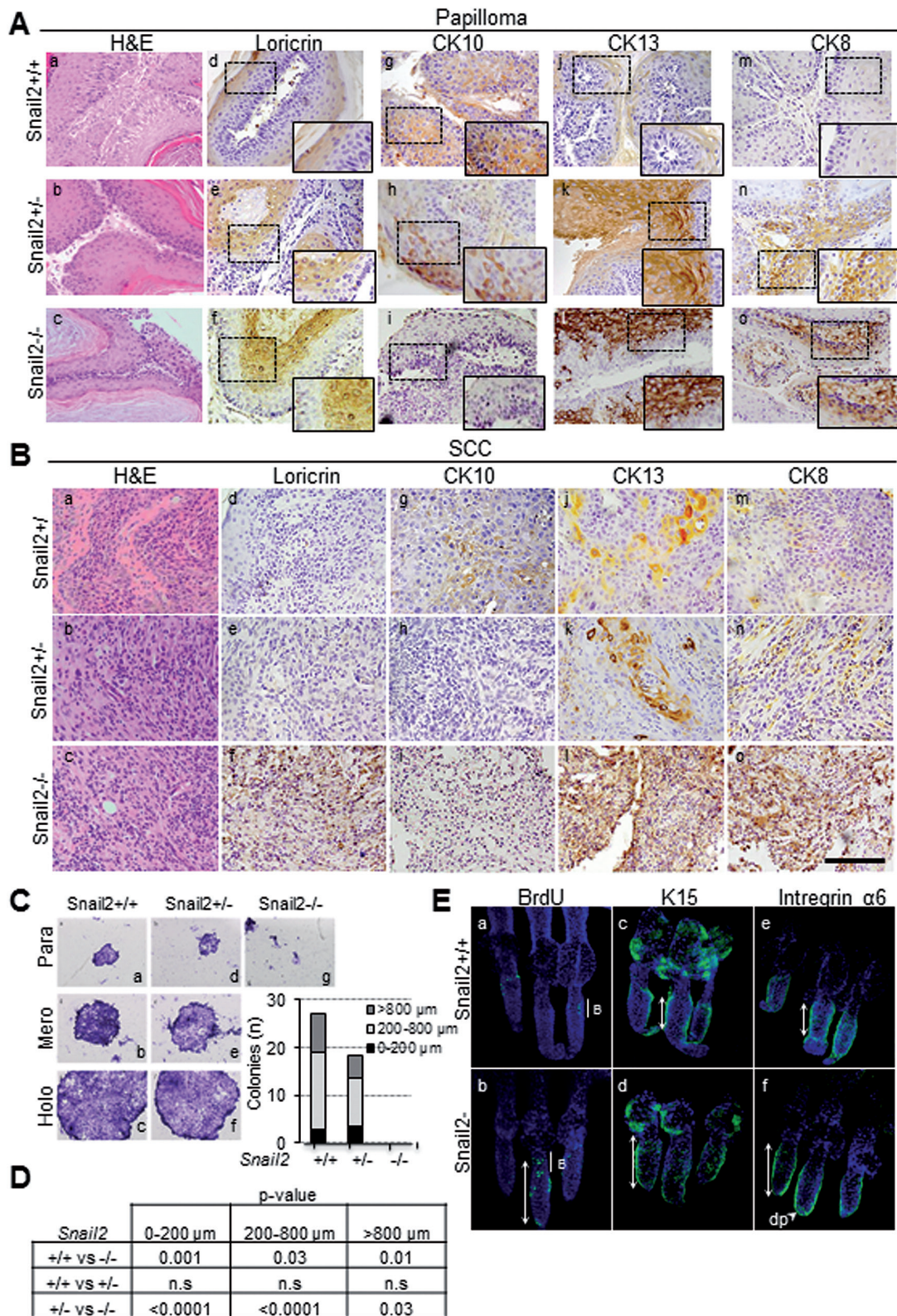


**Figure 3.** Analysis of differentiation markers in DMBA/TPA lesions, *in vitro* keratinocyte proliferation and label retaining cell (LRC) distribution. (A) and (B) Immunohistochemical analysis of differentiation markers in papillomas (A) and SCC (B) from the three *Snail2* genotypes. H&E images showing tumor histology are included in panels a–c. Representative images of loricrin (d–f), CK10 (g–i), CK13 (j–l) and CK8 (m–o) are presented. Bar, 500 µm. Amplified images of the indicated areas (squares) are included as insets. (C) Representative images of the different type of colonies generated by primary keratinocyte cultures (para, mero and holoclones) from newborn *Snail2*<sup>+/+</sup> (a–c), *Snail2*<sup>+/-</sup> (d–f) and *Snail2*<sup>-/-</sup> (g) mice. The number of colonies (n) of the indicated size in each *Snail2* genotype is shown in the right side diagram. (D) Statistical analyses (t-test) of the colony number in the three *Snail2* genotypes; n.s., non-significant. (E) Representative images of LRC labeling with BrdU (a and b), K15 (c and d) and α6 integrin (e and f) from *Snail2*<sup>+/+</sup> and *Snail2*<sup>-/-</sup> mice tail HF. The extension of LRC, and K15 and α6 expression in HF from the two *Snail2* genotypes is indicated by white double-arrows. B, bulge region; dp, dermal papilla.

microenvironment. To discriminate between those options, we first analyzed the *in vitro* proliferative potential of primary keratinocytes by clonogenic assays. Results showed that *Snail2*<sup>-/-</sup> primary keratinocyte cultures were not clonogenic (Figure 3C, g and D), whereas primary keratinocytes from *Snail2*<sup>+/+</sup> and *Snail2*<sup>+/-</sup> mice were able to form the three types of colonies: paraclones, meroclones and holoclones (Figure 3C, a–f and D). These data suggest that epidermal keratinocytes alone are not responsible for increased tumor burden and malignancy of *Snail2*<sup>-/-</sup> lesions. Because stem cells from the HF at the bulge region have been proposed as competent in the formation of epidermal tumors in response to environmental cues (32,37), we then investigated the influence of *Snail2* in the HF stem cell compartment. To this end, analysis of the label retaining cells population in *Snail2*<sup>-/-</sup> and *Snail2*<sup>+/+</sup> mice was performed. BrdU labeling, together with analyses of K15 and  $\alpha 6$  integrin, markers of HF stem cells (32,37) showed that *Snail2*<sup>-/-</sup> mice displayed an increased stem cell population not only restricted to the bulge but also extending to additional HF regions (Figure 3E, a, b, white double-head arrows). Extended expression of K15 and  $\alpha 6$  integrin stem cell markers was also observed in *Snail2*<sup>-/-</sup> HF (Figure 3E, c–f). These data suggest that *Snail2* deficiency alters the HF stem cell compartment that could be more prone to be mobilized and expanded under a proliferative or carcinogenic stimulus. In fact, analyses of the HF cycle by a classical clipping assay indicated that *Snail2* deletion markedly accelerates HF growth at the refractory telogen phase (P50); increased  $\beta$ -catenin expression in *Snail2*<sup>-/-</sup> HFs was also observed, together with higher expression of proliferation markers and diminished expression of stem cell markers (Supplementary Figure S4, available at Carcinogenesis Online) supporting the induction of the anagen phase by *Snail2* deletion. Collectively, these data suggest that epidermal stem or progenitor cells are more prone to respond to carcinogenic and proliferative stimuli in the absence of *Snail2* *in vivo*.

### Snail2 deletion promotes inflammation in tumor lesions

In order to gain insight into the environmental factors responsible for the increased malignancy of *Snail2*<sup>-/-</sup> lesions, a deeper histopathological analysis of skin tumors was performed. *Snail2*<sup>-/-</sup> lesions displayed abundant infiltrations of inflammatory cells that were not observed in wild-type mice (Figure 4A, upper, white arrowheads). This event prompted us to study the potential role of inflammation in tumor progression in *Snail2*<sup>-/-</sup> mice; to this end, we first analyzed the effect of dexamethasone treatment on skin tumor progression. *Snail2*<sup>+/+</sup> and *Snail2*<sup>-/-</sup> mice were subjected to the DMBA/TPA chemical carcinogenesis protocol, and when all the animals developed tumors (week 12), dexamethasone, or control PBS, was injected daily until the end of the experiment (week 18) (Figure 4B). *Snail2*<sup>+/+</sup> mice developed lower number of lesions (four versus nine at the end of the experiment) of smaller size and decreased malignant progression after dexamethasone treatment compared with controls (Figure 4B–D and Supplementary Table S4, available at Carcinogenesis Online). In contrast, the treatment of *Snail2*<sup>-/-</sup> mice with dexamethasone increased the number (36 lesions/mice) and size of lesions compared with control-treated mice (16 lesions/mice) (Figure 4B and C and Supplementary Table S4, available at Carcinogenesis Online). However, despite of this increase, histopathological analyses revealed that these lesions were mostly papillomas. Thus, this anti-inflammatory treatment resulted in a significant decrease in the incidence of SCC

in both *Snail2*<sup>-/-</sup> and wild-type mice (Figure 4D). These results led us to hypothesize that progression of *Snail2* null skin tumors to malignancy is inflammation-driven since the treatment with dexamethasone significantly decreased the percentage of SCC, without affecting the latency of the lesions. On the other hand, and unexpectedly, these blockade in the progression to SCCs in *Snail2*<sup>-/-</sup> resulted in an increase in the number of hyperplastic lesions or papillomas. Overall, these results uncovered that loss of *Snail2* leads to the recruitment of inflammatory cells in response to the skin carcinogenesis treatment that contribute to the progression to SCC.

To identify the inflammatory component modified in *Snail2*<sup>-/-</sup> mice, we explored if there were any changes in the populations of different immune cells in blood, BM and tumors by flow cytometry at the end of the standard carcinogenesis experiment. The results showed a significant higher proportion of myeloid (CD11b<sup>+</sup>/Gr-1<sup>+</sup>) cells in all samples from *Snail2*<sup>-/-</sup> mice compared with those from *Snail2*<sup>-/-</sup> and *Snail2*<sup>+/+</sup> mice (Figure 4E). Although not statistically significant, higher numbers of cytotoxic T (CD8<sup>+</sup>) and B (CD19<sup>+</sup>) lymphocytes were also detected in *Snail2*<sup>-/-</sup> lesions (Figure 4F).

Altogether, these data point to the involvement of the inflammatory response in *Snail2*<sup>-/-</sup> mice under the carcinogenesis treatment as a positive input to tumor progression.

### Loss of Snail2 induces the mobilization of hematopoietic cells during tumor progression

Because of the previous implication of *Snail2* in hematopoietic system homeostasis (14,15,17), we next decided to investigate whether *Snail2* deletion in the hematopoietic system could account for the observed alterations in tumor progression. To this end, BM cross-restitutions experiments were carried out generating *Snail2*<sup>+/+</sup> mice reconstituted with BM from null mutant mice or from wild-type mice as control (referred as *Snail2*<sup>+/+</sup>\_BMS*Snail2*<sup>-/-</sup>, *Snail2*<sup>+/+</sup>\_BMS*Snail2*<sup>+/+</sup>, respectively) (Supplementary Figure S5A, available at Carcinogenesis Online).

The results showed that the incidence of lesions did not change between both groups of animals (data not shown), but the tumor burden exhibited two different phases. At early stages, no differences were observed between both groups of reconstituted mice, but following 14 weeks post-initiation, *Snail2*<sup>+/+</sup>\_BMS*Snail2*<sup>-/-</sup> mice developed increased number and larger lesions compared with *Snail2*<sup>+/+</sup>\_BMS*Snail2*<sup>+/+</sup> mice (average of 30 versus 20 lesions/mouse at 20 weeks). The difference between the two groups was statistically significant between 16 and 20 weeks (Figure 5A and B and Supplementary Table S5, available at Carcinogenesis Online). The incidence of SCCs in the reconstituted mice, although not as evident as we observed for the parental null mice, was also higher in *Snail2*<sup>+/+</sup>\_BMS*Snail2*<sup>-/-</sup> (12% of SCC) compared with *Snail2*<sup>+/+</sup>\_BMS*Snail2*<sup>+/+</sup> mice (6% of SCC) (Supplementary Figure S5B and S5C, available at Carcinogenesis Online). Therefore, the reconstituted *Snail2*<sup>+/+</sup>\_BMS*Snail2*<sup>-/-</sup> mice mirror the tumor behavior of *Snail2*<sup>-/-</sup> mice (Figure 2B and C), strongly suggesting a link between *Snail2* deletion in the hematopoietic system and increased malignant progression.

Analysis of the myeloid component indicated that the CD11b<sup>+</sup>/Gr-1<sup>+</sup> cell population was significantly increased in blood, BM and tumors from *Snail2*<sup>+/+</sup>\_BMS*Snail2*<sup>-/-</sup> compared with control *Snail2*<sup>+/+</sup>\_BMS*Snail2*<sup>+/+</sup> mice (Figure 5C). Additionally, a significant increase in CD8<sup>+</sup> T cells and an increased content, although not statistically significant, of CD19<sup>+</sup> B lymphocytes and F4/80<sup>+</sup> macrophage populations were also detected in *Snail2*<sup>+/+</sup>\_BMS*Snail2*<sup>-/-</sup> tumor lesions (Figure 5D). To confirm the *Snail2* influence in the



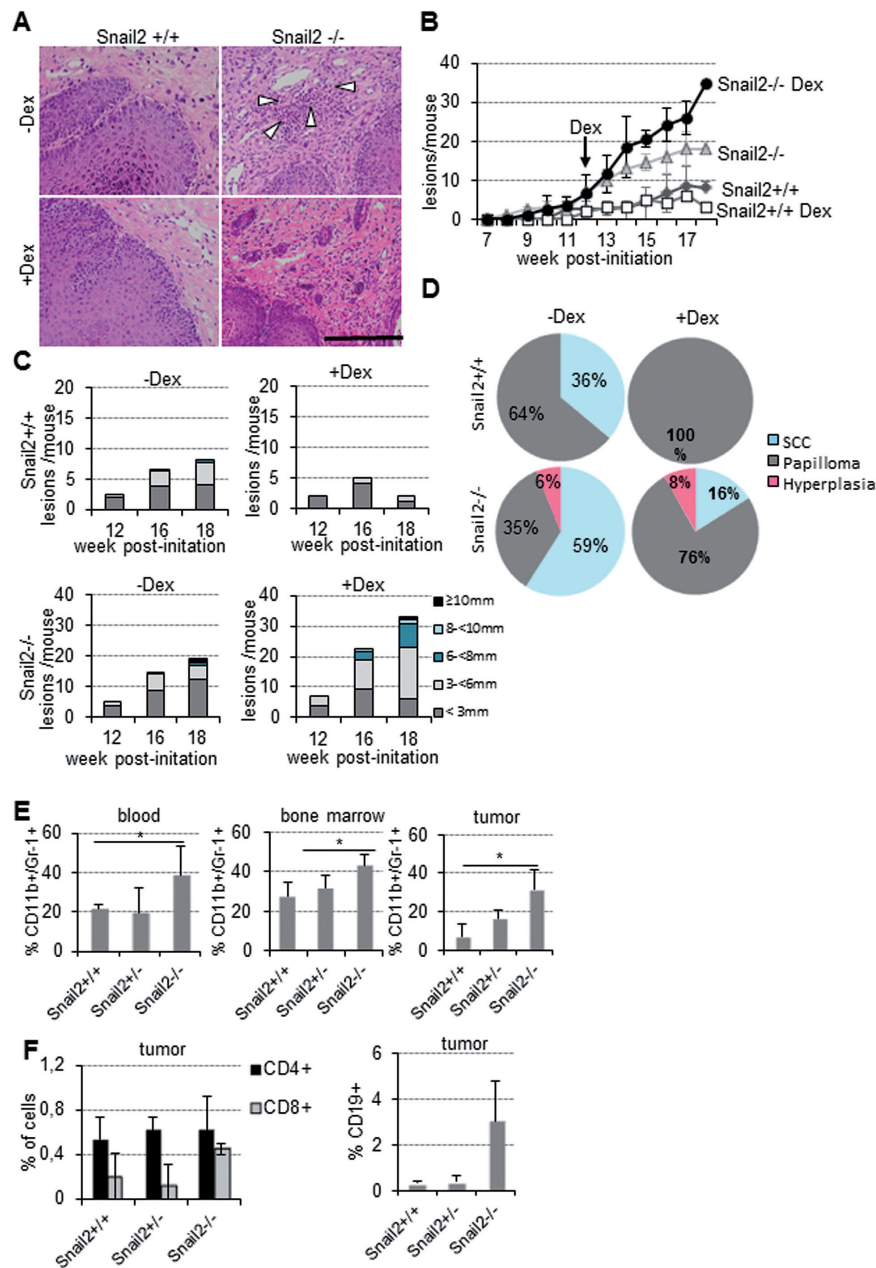


**Figure 4.** *Snail2* deletion induces a high inflammatory response in DMBA/TPA skin carcinogenesis. (A) H&E of *Snail2*<sup>+/+</sup> and *Snail2*<sup>-/-</sup> lesions from control (a and b) and after dexamethasone (Dex) treatment (c and d) of *Snail2*<sup>+/+</sup> and *Snail2*<sup>-/-</sup> mice subjected to skin carcinogenesis. White arrowheads denote the inflammatory component in untreated *Snail2*<sup>-/-</sup> lesions. (B) Tumor burden of *Snail2*<sup>+/+</sup> and *Snail2*<sup>-/-</sup> mice control (dimethyl sulfoxide) and treated with Dex at 12 weeks post-initiation; n = 7 per genotype. Only one mouse survived up to 18 weeks from the Dex-treated *Snail2*<sup>-/-</sup> group. (C) Tumor size at the indicated times post-initiation represented as the mean number of lesions per mouse with the indicated diameter for each condition in *Snail2*<sup>+/+</sup> and *Snail2*<sup>-/-</sup> mice. (D) Distribution of the lesions generated by DMBA/TPA treatment classified as hyperplasia, papillomas and SCC in *Snail2*<sup>+/+</sup> and *Snail2*<sup>-/-</sup> treated or untreated with Dex. (E) Analysis of the CD11b<sup>+</sup>/Gr-1<sup>+</sup> myeloid population in blood, BM and tumors from mice treated with DMBA/TPA (n = 6 per each genotype). Double positive cells are significantly increased in *Snail2*<sup>-/-</sup> mice. (F) Analysis of CD4<sup>+</sup>, CD8<sup>+</sup> and CD19<sup>+</sup> populations in tumor lesions. CD8<sup>+</sup> and CD19<sup>+</sup> population were increased in *Snail2*<sup>-/-</sup> tumors. \*P ≤ 0.05.

inflammatory component observed in these results, we performed a reverse BM cross-reconstitution assay generating *Snail2*<sup>-/-</sup> mice transplanted with BM from *Snail2*<sup>+/+</sup>, *Snail2*<sup>-/-</sup> or *Snail2*<sup>+/-</sup> mice (*Snail2*<sup>-/-</sup>\_BMS*Snail2*<sup>+/+</sup>, *Snail2*<sup>-/-</sup>\_BMS*Snail2*<sup>+/-</sup> and *Snail2*<sup>-/-</sup>\_BMS*Snail2*<sup>-/-</sup>) (Supplementary Figure S5D, available at Carcinogenesis Online) and subjected to skin chemical carcinogenesis. The sensitivity of *Snail2*<sup>-/-</sup> mice to radiation (14–16) strongly decreased the survival of transplanted mice throughout the carcinogenesis experiment, even when those mice were irradiated at a sublethal dosage. Only 3–4 out of 6–8 mice from the different cross-reconstituted

groups survived. Despite the low number of surviving mice, the obtained results strongly suggested that mice reconstituted with *Snail2*<sup>-/-</sup> BM exhibit a behavior similar to control *Snail2*<sup>-/-</sup> mice. Thus, a similar tumor incidence was detected in the three cross-reconstituted models, although tumor initiation was delayed in *Snail2*<sup>-/-</sup>\_BMS*Snail2*<sup>+/+</sup> (data not shown) as previously observed in *Snail2*<sup>-/-</sup> mice. Regarding tumor burden, the behavior (Figure 6A) was reminiscent of that found in the BM donor mice (compare with Figure 2B). *Snail2*<sup>-/-</sup>\_BMS*Snail2*<sup>+/-</sup> mice significantly reduced the tumor burden (average 10 lesions/mouse) and size of the

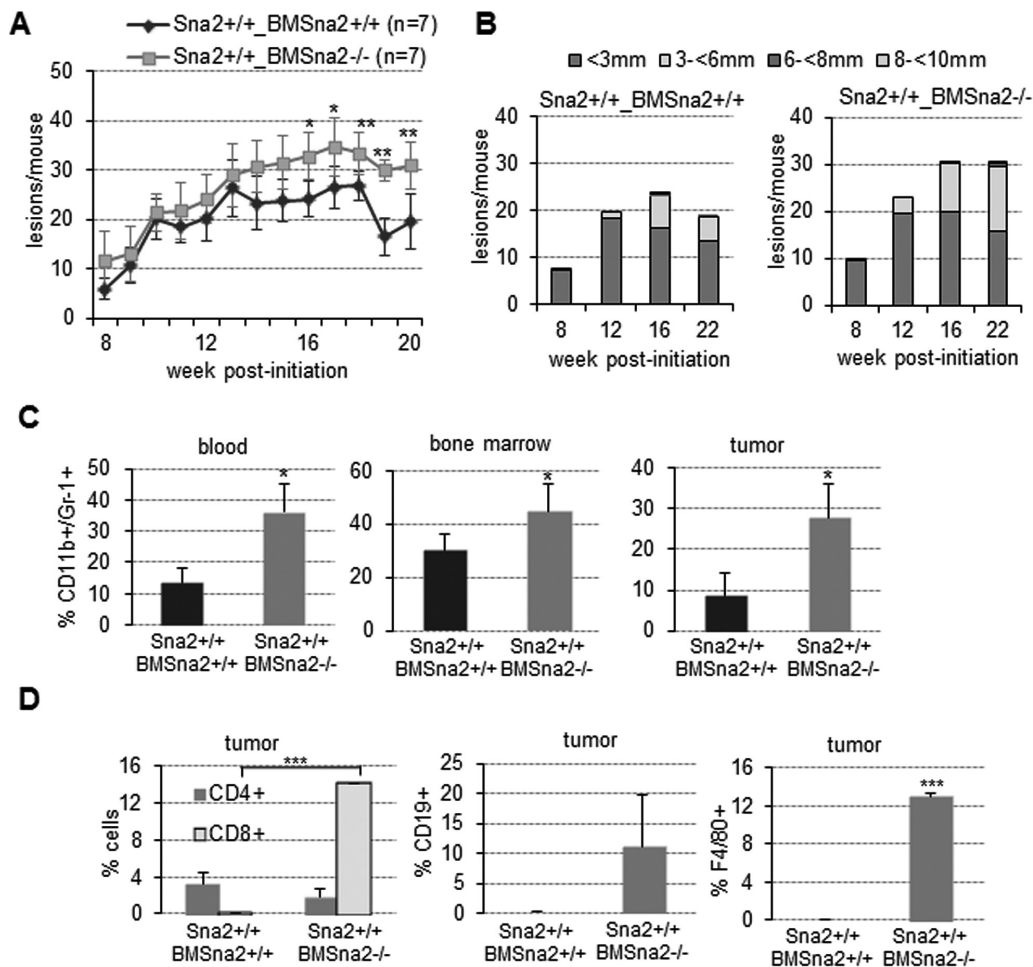


**Figure 5.** Effect of *Snail2* constitutive deletion in hematopoietic progenitors during skin chemical carcinogenesis. (A) Tumor burden (lesions/mouse) showing the differences between *Snail2*<sup>+/+</sup>\_BMS*Snail2*<sup>-/-</sup> and *Snail2*<sup>+/+</sup>\_BMS*Snail2*<sup>+/+</sup> mice after DMBA/TPA treatment; n = 7 mice per experimental group. \*P < 0.05. (B) Tumor size comparison between *Snail2*<sup>+/+</sup>\_BMS*Snail2*<sup>+/+</sup> and *Snail2*<sup>+/+</sup>\_BMS*Snail2*<sup>-/-</sup> lesions. (C) Flow cytometry analysis of CD11b<sup>+</sup>/Gr-1<sup>+</sup> population in blood, BM and tumors in *Snail2*<sup>+/+</sup>\_BMS*Snail2*<sup>+/+</sup> and *Snail2*<sup>+/+</sup>\_BMS*Snail2*<sup>-/-</sup> mice after DMBA/TPA treatment. (D) Flow cytometry analysis of CD4<sup>+</sup>, CD8<sup>+</sup>, CD19<sup>+</sup> and F4/80<sup>+</sup> cell populations of *Snail2*<sup>+/+</sup>\_BMS*Snail2*<sup>+/+</sup> and *Snail2*<sup>+/+</sup>\_BMS*Snail2*<sup>-/-</sup> tumors. (C) and (D) n = 4 and 5 for *Snail2*<sup>+/+</sup>\_BMS*Snail2*<sup>+/+</sup> and *Snail2*<sup>+/+</sup>\_BMS*Snail2*<sup>-/-</sup> mice, respectively. t-Test, \*P < 0.05, \*\*0.001 < P < 0.005, \*\*\*P < 0.001.

lesions as compared with *Snail2*<sup>-/-</sup>\_BMS*Snail2*<sup>-/-</sup> (average 35 lesions/mouse) that also showed a trend to increased number of lesions and of larger size as compared with *Snail2*<sup>-/-</sup>\_BMS*Snail2*<sup>+/+</sup> mice (average 23 lesions/mouse) (Figure 6A and B, and Supplementary Table S6, available at Carcinogenesis Online). A similar trend toward increased SCC progression was detected in lesions from *Snail2*<sup>-/-</sup>\_BMS*Snail2*<sup>-/-</sup> mice compared with the other two groups (Supplementary Figure S5D and S5E, available at Carcinogenesis Online). Analyses of the myeloid component in blood, BM and tumor samples of the *Snail2*<sup>-/-</sup> BM reconstituted mice, indicated an increased, but not statistically significant, CD11b<sup>+</sup>/Gr-1<sup>+</sup> population in *Snail2*<sup>-/-</sup>\_BMS*Snail2*<sup>-/-</sup> mice compared with the other two models (Figure 6C), similar to that detected in the parental *Snail2*<sup>-/-</sup> mice (compare with Figure 4D).

Altogether, these results support that *Snail2* deletion in the hematopoietic system leads to an elevated inflammatory response that favors a pro-tumor microenvironment to increase the number, size and progression of skin lesions.

## Discussion

In the present work, we have characterized the role of *Snail2* in skin physiology and found that *Snail2* is essential for survival

and proliferation of keratinocytes *in vitro*. This is in accordance with the reported survival role of *Snail2* in other cellular systems (9,29,38–41). On the other hand, the study of *in vivo* skin response to wounding and TPA-induced hyperproliferation showed that *Snail2* deficiency impairs re-epithelialization, in agreement with previous results (8,10,42), and decreases the hyperproliferation response. Furthermore, the expression of epidermal terminal differentiation markers was altered in *Snail2* null mice, suggesting that *Snail2* is a key regulator of keratinocyte proliferation and differentiation.

*Snail2* is an EMT factor related with tumor progression, stemness and chemoresistance among other processes (2), and therefore it was expected that *Snail2* deletion would negatively affect tumor development and/or progression. Nevertheless, and unexpectedly, constitutive *Snail2* deletion fosters the pro-tumorigenic response to skin chemical carcinogenesis with an increase in the number, size and malignant progression of the lesions. These results contrast with a previous report on the response of *Snail2* null mice to ultraviolet radiation-induced skin carcinogenesis showing decreased tumor burden and progression than wild-type mice (43). Although these differences could be partly explained by the different genetic backgrounds of the null mice used in both studies, they also suggest that

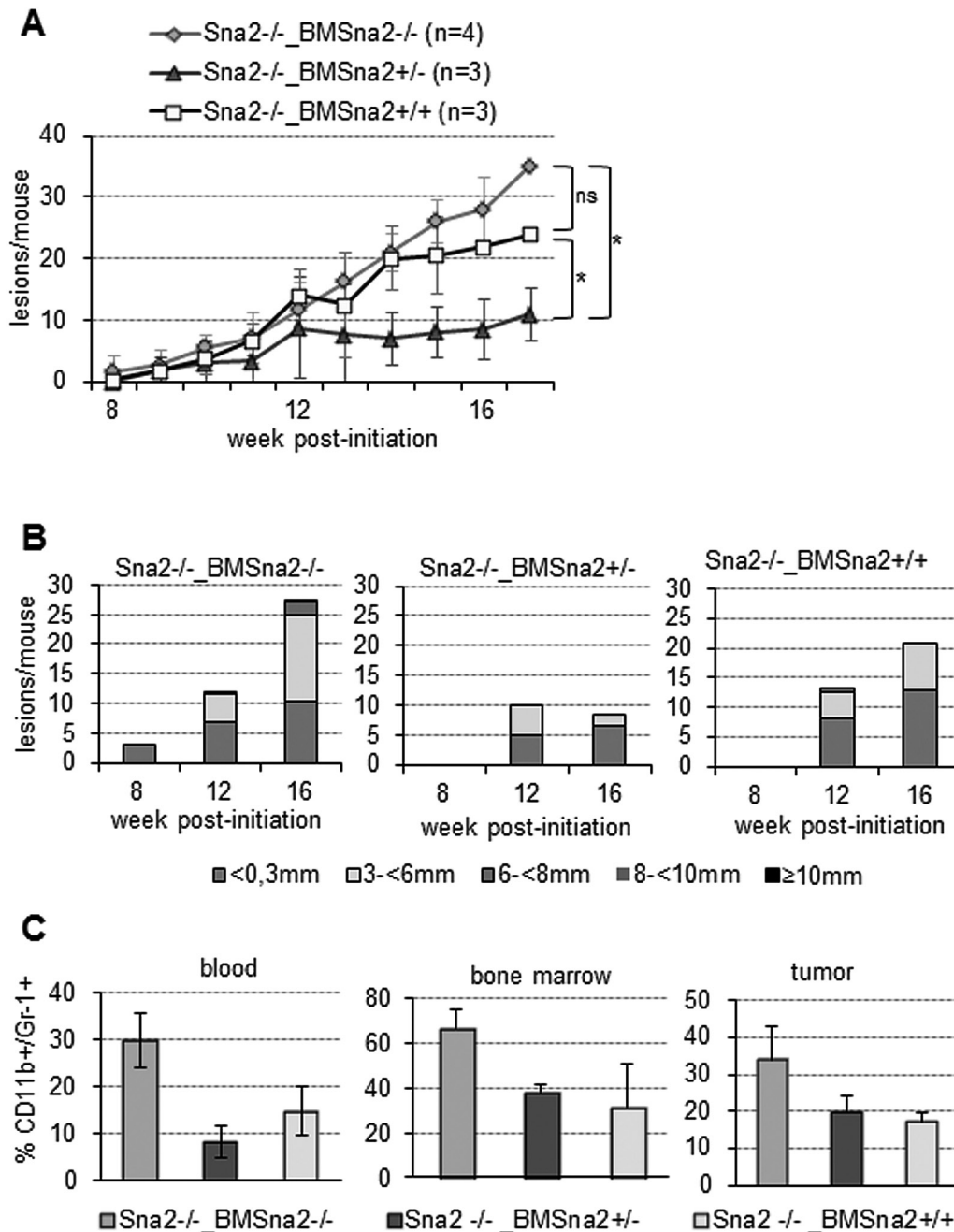


**Figure 6.** *Snail2* wild-type BM reconstitution avoids the *Snail2*<sup>-/-</sup> phenotype after chemical carcinogenesis. (A) Tumor burden (lesions/mouse) of *Snail2*<sup>-/-</sup> mice reconstituted with BM from *Snail2*<sup>-/-</sup> (*Snail2*<sup>-/-</sup>\_BMS*Snail2*<sup>-/-</sup>, n = 4), *Snail2*<sup>+/-</sup> (*Snail2*<sup>-/-</sup>\_BMS*Snail2*<sup>+/-</sup>, n = 3) and *Snail2*<sup>+/+</sup> (*Snail2*<sup>-/-</sup>\_BMS*Snail2*<sup>+/+</sup>, n = 3) mice after DMBA/TPA treatment. t-Test, \*P ≤ 0.05; n.s. not significant. (B) Tumor size at the indicated times post-initiation represented as the mean number of lesions per mouse with the indicated diameter for each condition in *Snail2*<sup>-/-</sup>\_BMS*Snail2*<sup>-/-</sup>, *Snail2*<sup>-/-</sup>\_BMS*Snail2*<sup>+/-</sup> and *Snail2*<sup>-/-</sup>\_BMS*Snail2*<sup>+/+</sup> mice. (C) Flow cytometry analysis for CD11b<sup>+</sup>/Gr-1<sup>+</sup> cells showing lower levels of myeloid population in *Snail2*<sup>-/-</sup>\_BMS*Snail2*<sup>+/-</sup> and *Snail2*<sup>-/-</sup>\_BMS*Snail2*<sup>+/+</sup> mice in blood, BM and tumors compared with control *Snail2*<sup>-/-</sup>\_BMS*Snail2*<sup>-/-</sup> mice. n = 3 per experimental group.

they could be related to the influence of *Snail2* in the inflammatory response to ultraviolet radiation (11). Indeed, the inability of *Snail2*<sup>-/-</sup> keratinocytes to proliferate *in vitro* suggests that other factors from the tumor microenvironment and/or tumor-stroma interactions could be enhancing lesion development and progression in a non-cell autonomous fashion. Noticeably, stem cells from the HF bulge region of *Snail2* null mice are apparently increased in number and show a wider localization compared with wild-type mice, suggesting that

this population could contribute to the increased response to the carcinogenic insult in *Snail2* deficient mice, as observed in other genetic contexts (32,37). Interestingly, we observed that lesions from *Snail2*<sup>-/-</sup> mice had a high inflammatory component not present in those derived from *Snail2*<sup>+/+</sup> mice. Moreover, treatment with dexamethasone during chemical skin carcinogenesis exacerbated the number of lesions developed by *Snail2*<sup>-/-</sup> mice but blocked their progression to SCCs. Altogether, the data suggest that dexamethasone treatment in *Snail2*<sup>-/-</sup> mice blocks

antitumor inflammatory processes while favoring a pro-inflammatory response, likely due to alterations in the *Snail2*<sup>-/-</sup> inflammatory system. The immune response may initially attempt to eliminate cancer cells, but paradoxically this response can be pro-tumorigenic (44). For example, cells of the myeloid lineage, such as macrophages (45) and neutrophils (46), can promote tumor growth. Immature myeloid cells (IMCs) can also promote tumor growth directly or by acting as myeloid-derived suppressor cells (47). Other inflammatory populations have also been related with this pro-tumorigenic activity, such as a subgroup of the CD8+ T-cell population (48). Interestingly, the analyses of myeloid precursors (CD11b<sup>+</sup>/Gr-1<sup>+</sup> cells) in mice subjected to skin carcinogenesis revealed an increment of this population in *Snail2*<sup>-/-</sup> blood, BM and tumors compared with *Snail2*<sup>+/+</sup> and *Snail2*<sup>+/-</sup> samples. Moreover, an increase in other pro-inflammatory populations like B lymphocytes and cytotoxic T cells was also detected within *Snail2*<sup>-/-</sup> tumors.

The above results suggest that *Snail2* deletion in hematopoietic progenitors promotes the mobilization and accumulation of myeloid precursors in the tumor lesions. Remarkably, BM reconstitution assays showed that reconstituted *Snail2*<sup>+/+</sup><sub>BMSnail2</sub><sup>-/-</sup> mice exhibited a similar number and larger lesions than their *Snail2*<sup>+/+</sup><sub>BMSnail2</sub><sup>+/+</sup> counterparts, mimicking the behavior of *Snail2*<sup>-/-</sup> mice. Importantly, *Snail2*<sup>+/+</sup><sub>BMSnail2</sub><sup>-/-</sup> mice also show an increase in myeloid precursors and other inflammatory populations within the tumors (CD19+, CD8+ and F4/80+ cells) compared with controls. The reverse reconstitution experiments in *Snail2*<sup>-/-</sup> mice (*Snail2*<sup>-/-</sup><sub>BMSnail2</sub><sup>+/+</sup>) resulted in the complementary effect, thus mimicking the behavior of *Snail2* wild-type mice, regarding decreased tumor development and myeloid recruitment compared with *Snail2* null mice. These data indicate that the absence of *Snail2* in hematopoietic precursors is responsible of the pro-tumorigenic response of *Snail2* null mice to skin chemical carcinogenesis, perhaps also due to alteration in the barrier function. *In vitro* culture of *Snail2*<sup>-/-</sup> keratinocytes in the presence of BM-conditioned media isolated from either control or *Snail2*<sup>-/-</sup> mice did not rescue their inability to grow in clonogenic assays (data not shown). These data suggest that the pro-tumorigenic influence of *Snail2* deletion in the hematopoietic compartment is only manifested in *in vivo* context rather than on *in vitro* proliferation. Together, the present data support a main role of *Snail2* in keratinocyte-hematopoietic interactions and/or other components of the tumor microenvironment regulating tumor progression. Myeloid precursors are a heterogeneous population of cells that consists of myeloid progenitor cells and IMCs. In healthy individuals, IMCs generated in the BM quickly differentiate into mature granulocytes, macrophages and dendritic cells. In contrast, in pathological conditions, such as cancer, a partial block in the differentiation of IMCs into mature myeloid cells results in the expansion of this population (46,47). Myeloid precursors can also differentiate into tumor-associated macrophages within the tumor microenvironment. Furthermore, signaling pathways important for myeloid precursors expansion like the JAK/STAT pathway (47,49) are also inducers of EMT factors, such as *Snail2*. Thus, the absence of *Snail2* may compromise the expected behavior of myeloid precursors, mirroring the described effect of *Snail2* deficiency in hematopoiesis (14,16,17). The tumor-promoting role of CD11b<sup>+</sup>/Gr-1<sup>+</sup> myeloid precursors has been previously reported in a variety of studies (47,49–51) and proposed to exert this effect by increasing the Wnt/ $\beta$ -catenin signaling in neighboring epithelial cells via the secretion of Wnt ligands and the Wnt agonist POSTN by the stroma (34). Interestingly, increased nuclear localization of  $\beta$ -catenin and upregulation

of several Wnt ligands, particularly Wnt4, and POSTN were detected in *Snail2*<sup>-/-</sup> lesions as compared with wild-type and *Snail2*<sup>+/-</sup> lesions, strongly suggesting that the dermal stroma of *Snail2* null mice may be primed to facilitate the pro-tumorigenic function of CD11b<sup>+</sup>/Gr-1<sup>+</sup> myeloid cells.

In contrast to *Snail2* null mice, heterozygous animals are less prone to skin tumor development and progression than wild-type mice, and this behavior was reproduced in reconstituted *Snail2*<sup>-/-</sup><sub>BMSnail2</sub><sup>+/-</sup> mice. Interestingly, *Snail2*<sup>+/-</sup> papillomas do not progress to SCC, despite the fact that they show a pre-malignant potential according to the expression of differentiation markers. The observed increased apoptosis in *Snail2*<sup>+/-</sup> papillomas in the absence of increased proliferation detected in *Snail2*<sup>-/-</sup> (Figure 2E and F) can, at least partly, explain the behavior of *Snail2*<sup>+/-</sup> lesions. On the other hand, the observed decreased expression of some EMT transcription factors, like *Zeb1* in skin from *Snail2*<sup>+/-</sup> mice (Supplementary Figure S1, available at Carcinogenesis Online), also suggests that *Zeb1* might participate in skin carcinogenesis progression, as reported in melanoma (52), and its partial repression contribute to the decreased response of *Snail2* heterozygous mice. Noticeably, the CD11b<sup>+</sup>/Gr-1<sup>+</sup> population is not increased in BM, blood or tumors from *Snail2*<sup>-/-</sup> mice, showing also no changes in  $\beta$ -catenin activation compared with wild-type mice. These data indicate that a decrease in *Snail2* dosage protects against tumor development and progression probably by blocking myeloid precursors recruitment and favoring their differentiation and anti-inflammatory actions, whereas complete *Snail2* absence triggers the opposite response in the myeloid population providing a permissive environment for tumor onset and progression during chemical carcinogenesis.

## Supplementary material

Supplementary Tables S1–S6 and Supplementary Figures S1–S5 can be found at <http://carcin.oxfordjournals.org/>

## Funding

Spanish Ministry of Science and Innovation (SAF2010-21143; Consolider-Ingenio 2007-CS00017; SAF2013-44739R); Worldwode Research Cancer (formerly AICR: Association for International Cancer Research) (12-1057); Instituto de Salud Carlos III (RETIC-RD12/0036/0007) to A.C. and F.P.; Comunidad de Madrid (S2010/BMD-2302 to A.C. and G.M.-B.); National Institutes of Health (NIH R01HD034883 to T.G.).

## Acknowledgements

The authors thank Francesca Antonucci for help in the clonogenic assays and members of A.C.'s lab for helpful discussions. *Conflict of Interest Statement*: None declared.

## References

- Nieto, M.A. (2002) The snail superfamily of zinc-finger transcription factors. *Nat. Rev. Mol. Cell Biol.*, 3, 155–166.
- Nieto, M.A. (2011) The ins and outs of the epithelial to mesenchymal transition in health and disease. *Annu. Rev. Cell Dev. Biol.*, 27, 347–376.
- Thiery, J.P. et al. (2009) Epithelial-mesenchymal transitions in development and disease. *Cell*, 139, 871–890.
- Sefton, M. et al. (1998) Conserved and divergent roles for members of the Snail family of transcription factors in the chick and mouse embryo. *Development*, 125, 3111–3121.
- Oram, K.F. et al. (2003) Slug expression during organogenesis in mice. *Anat. Rec. A Discov. Mol. Cell. Evol. Biol.*, 271, 189–191.

6. Jiang, R. et al. (1998) Genomic organization, expression and chromosomal localization of the mouse Slug (Slugh) gene. *Biochim. Biophys. Acta*, 1443, 251–254.
7. Parent, A.E. et al. (2004) The developmental transcription factor slug is widely expressed in tissues of adult mice. *J. Histochem. Cytochem.*, 52, 959–965.
8. Hudson, L.G. et al. (2009) Cutaneous wound reepithelialization is compromised in mice lacking functional Slug (Snai2). *J. Dermatol. Sci.*, 56, 19–26.
9. Newkirk, K.M. et al. (2008) Microarray analysis demonstrates a role for Slug in epidermal homeostasis. *J. Invest. Dermatol.*, 128, 361–369.
10. Savagner, P. et al. (2005) Developmental transcription factor slug is required for effective re-epithelialization by adult keratinocytes. *J. Cell. Physiol.*, 202, 858–866.
11. Newkirk, K.M. et al. (2008) The acute cutaneous inflammatory response is attenuated in Slug-knockout mice. *Lab. Invest.*, 88, 831–841.
12. Carver, E.A. et al. (2001) The mouse snail gene encodes a key regulator of the epithelial-mesenchymal transition. *Mol. Cell. Biol.*, 21, 8184–8188.
13. Jiang, R. et al. (1998) The Slug gene is not essential for mesoderm or neural crest development in mice. *Dev. Biol.*, 198, 277–285.
14. Inoue, A. et al. (2002) Slug, a highly conserved zinc finger transcriptional repressor, protects hematopoietic progenitor cells from radiation-induced apoptosis *in vivo*. *Cancer Cell*, 2, 279–288.
15. Pérez-Losada, J. et al. (2002) Zinc-finger transcription factor Slug contributes to the function of the stem cell factor c-kit signaling pathway. *Blood*, 100, 1274–1286.
16. Pérez-Losada, J. et al. (2003) The radioresistance biological function of the SCF/kit signaling pathway is mediated by the zinc-finger transcription factor Slug. *Oncogene*, 22, 4205–4211.
17. Sun, Y. et al. (2010) Slug deficiency enhances self-renewal of hematopoietic stem cells during hematopoietic regeneration. *Blood*, 115, 1709–1717.
18. Moreno-Bueno, G. et al. (2008) Transcriptional regulation of cell polarity in EMT and cancer. *Oncogene*, 27, 6958–6969.
19. Nieto, M.A. et al. (2012) The epithelial-mesenchymal transition under control: global programs to regulate epithelial plasticity. *Semin. Cancer Biol.*, 22, 361–368.
20. Savagner, P. et al. (1997) The zinc-finger protein slug causes desmosome dissociation, an initial and necessary step for growth factor-induced epithelial-mesenchymal transition. *J. Cell Biol.*, 137, 1403–1419.
21. Hajra, K.M. et al. (2002) The SLUG zinc finger protein represses E-cadherin in breast cancer cells. *Cancer Res.*, 62, 1613–1618.
22. Bolós, V. et al. (2003) The transcription factor Slug represses E-cadherin expression and induces epithelial to mesenchymal transitions: a comparison with Snail and E47 repressors. *J. Cell Sci.*, 116(Pt 3), 499–511.
23. Cobaleda, C. et al. (2007) Function of the zinc-finger transcription factor SNAI2 in cancer and development. *Annu. Rev. Genet.*, 41, 41–61.
24. Peinado, H. et al. (2007). Snail, Zeb and bHLH factors in tumour progression: an alliance against the epithelial phenotype? *Nat. Rev. Cancer*, 7, 415–428.
25. Martin, T.A. et al. (2005) Expression of the transcription factors snail, slug, and twist and their clinical significance in human breast cancer. *Ann. Surg. Oncol.*, 12, 488–496.
26. Uchikado, Y. et al. (2005) Slug Expression in the E-cadherin preserved tumors is related to prognosis in patients with esophageal squamous cell carcinoma. *Clin. Cancer Res.*, 11, 1174–1180.
27. Proia, T.A. et al. (2011) Genetic predisposition directs breast cancer phenotype by dictating progenitor cell fate. *Cell Stem Cell*, 8, 149–163.
28. Guo, W. et al. (2012) Slug and Sox9 cooperatively determine the mammary stem cell state. *Cell*, 148, 1015–1028.
29. Kim, S. et al. (2014) Slug promotes survival during metastasis through suppression of Puma-mediated apoptosis. *Cancer Res.*, 74, 3695–3706.
30. Moreno-Bueno, G. et al. (2009) The morphological and molecular features of the epithelial-to-mesenchymal transition. *Nat. Protoc.*, 4, 1591–1613.
31. Conacci-Sorrell, M. et al. (2002) The cadherin-catenin adhesion system in signaling and cancer. *J. Clin. Invest.*, 109, 987–991.
32. Malanchi, I. et al. (2008) Cutaneous cancer stem cell maintenance is dependent on beta-catenin signalling. *Nature*, 452, 650–653.
33. Patturajan, M. et al. (2002) DeltaNp63 induces beta-catenin nuclear accumulation and signaling. *Cancer Cell*, 1, 369–379.
34. Malanchi, I. et al. (2012) Interactions between cancer stem cells and their niche govern metastatic colonization. *Nature*, 481, 85–89.
35. Gimenez-Conti, I. et al. (1990) Early expression of type I K13 keratin in the progression of mouse skin papillomas. *Carcinogenesis*, 11, 1995–1999.
36. Caulín, C. et al. (1993) Changes in keratin expression during malignant progression of transformed mouse epidermal keratinocytes. *Exp. Cell Res.*, 204, 11–21.
37. da Silva-Diz, V. et al. (2013) Progeny of Lgr5-expressing hair follicle stem cell contributes to papillomavirus-induced tumor development in epidermis. *Oncogene*, 32, 3732–3743.
38. Kurrey, N.K. et al. (2009) Snail and slug mediate radioresistance and chemoresistance by antagonizing p53-mediated apoptosis and acquiring a stem-like phenotype in ovarian cancer cells. *Stem Cells*, 27, 2059–2068.
39. Leroy, P. et al. (2007) Slug is required for cell survival during partial epithelial-mesenchymal transition of HGF-induced tubulogenesis. *Mol. Biol. Cell*, 18, 1943–1952.
40. Wu, W.S. et al. (2005) Slug antagonizes p53-mediated apoptosis of hematopoietic progenitors by repressing puma. *Cell*, 123, 641–653.
41. Zhang, C. et al. (2009) Unexpected functional redundancy between Twist and Slug (Snail2) and their feedback regulation of NF-kappaB via Nodal and Cerberus. *Dev. Biol.*, 331, 340–349.
42. Arnoux, V. et al. (2008) Erk5 controls Slug expression and keratinocyte activation during wound healing. *Mol. Biol. Cell*, 19, 4738–4749.
43. Newkirk, K.M. et al. (2007) Snai2 expression enhances ultraviolet radiation-induced skin carcinogenesis. *Am. J. Pathol.*, 171, 1629–1639.
44. Coussens, L.M. et al. (2002) Inflammation and cancer. *Nature*, 420, 860–867.
45. Allavena, P. et al. (2008) The inflammatory micro-environment in tumor progression: the role of tumor-associated macrophages. *Crit. Rev. Oncol. Hematol.*, 66, 1–9.
46. Fridlender, Z.G. et al. (2009) Polarization of tumor-associated neutrophil phenotype by TGF-beta: “N1” versus “N2” TAN. *Cancer Cell*, 16, 183–194.
47. Gabrilovich, D.I. et al. (2009) Myeloid-derived suppressor cells as regulators of the immune system. *Nat. Rev. Immunol.*, 9, 162–174.
48. Kwong, B.Y. et al. (2010) Molecular analysis of tumor-promoting CD8+ T cells in two-stage cutaneous chemical carcinogenesis. *J. Invest. Dermatol.*, 130, 1726–1736.
49. Nefedova, Y. et al. (2005) Regulation of dendritic cell differentiation and antitumor immune response in cancer by pharmacologic-selective inhibition of the janus-activated kinase 2/signal transducers and activators of transcription 3 pathway. *Cancer Res.*, 65, 9525–9535.
50. Elinav, E. et al. (2013) Inflammation-induced cancer: crosstalk between tumours, immune cells and microorganisms. *Nat. Rev. Cancer*, 13, 759–771.
51. Di Piazza, M. et al. (2012) Loss of cutaneous TSLP-dependent immune responses skews the balance of inflammation from tumor protective to tumor promoting. *Cancer Cell*, 22, 479–493.
52. Caramel, J. et al. (2013) A switch in the expression of embryonic EMT-inducers drives the development of malignant melanoma. *Cancer Cell*, 24, 466–480.